ACS OMEGA

http://pubs.acs.org/journal/acsodf

Article

Plasma Atomization of Strontium Chloride Powder by a Supersonic Plasma Jet and Measurement of Its Efficiency Using Diode Laser Absorption Spectroscopy

Akira Kuwahara,* Yasuaki Aiba, and Makoto Matsui

Cite This: *ACS Omega* 2021, 6, 11750−11755

Read Online

ACCESS | Metrics & More | Article Recommendations | Supporting Information

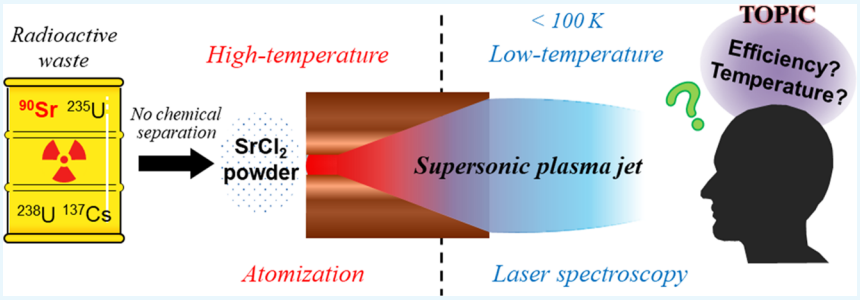

ABSTRACT: Direct elemental and isotope analyses of solid samples have attracted considerable interest due to their potential role in preventing serious accidents at nuclear facilities. We previously developed an analytical method for detecting radioactive isotopes, combining diode laser absorption spectroscopy with a supersonic plasma jet. Its basic performance, that is, the detection limit as well as the translational temperature upstream and downstream of the supersonic nozzle, was investigated using stable Xe isotopes. The developed apparatus could atomize a solid sample and reduce the translational temperature for isotope identification. For direct isotope analysis, translational temperature and atomization efficiency during powder feeding are remarkably important. In the present study, a novel approach for the atomization of Sr powder samples containing isotopes with highly radiotoxic radionuclides is described. We found that the temperature of Sr atoms in the supersonic plasma jet decreased to approximately 85 K, which is comparable with the slight isotope shift of ^{88}Sr−^{90}Sr due to the difference in mass number. Moreover, based on the measured atomic number density and flow velocity, the atomization efficiency was found to be 10.4 ± 1.8%. The results of this study and further improvements in the efficiency can lead to the development of powerful tools for the rapid analysis of solid samples, particularly those contaminated with highly radioactive species, without the necessity for complex chemical separation.

INTRODUCTION

Direct elemental and isotope analyses of radioactive waste are essential to confirm its safety, conduct environmental monitoring, and prevent severe accidents during the operation and decommissioning of nuclear facilities.[1−3] In a nuclear reactor, various radionuclides generated by nuclear fission, radioactivation, and atomic disintegration must be quantified to ensure long storage safety.[1] ^{90}Sr (half-life of 30 years) emits beta radiation with an energy maximum of 0.54 MeV. It is the most prevalent radiotoxic nuclide in fission products, and its yield is relatively high (approximately 6%).[4] Sr isotope analysis has been conventionally performed via inductively coupled plasma mass spectrometry (ICP−MS).[5,6] Nevertheless, a commercial ICP−MS apparatus is not suitable for the identification of ^{90}Sr from its daughter and grandchild nuclides (i.e., ^{90}Y and ^{90}Zr, respectively). Thus, in the case of ICP−MS, chemical separation, which typically takes 2−4 weeks, is necessary to prevent isobaric interference.[1,7]

Furthermore, laser spectroscopy techniques using laser ablation exhibit high wavelength selectivity and can be employed for the rapid identification of radioactive elements without the need for chemical separation. A tunable diode laser with a narrow line width can be used to distinguish isotope shifts based on the mass number.[8−15] Notably, laser ablation absorption spectroscopy (LAAS) has been developed for the rapid analysis of solid samples. Several recent studies describe the plasma plume dynamics and optimization of the LAAS conditions for direct isotope analysis.[10,16] However, upon irradiation of the surface with an intense laser beam to atomize a solid sample, the translational temperatures of molecules and

Received: February 28, 2021
Accepted: April 12, 2021
Published: April 22, 2021

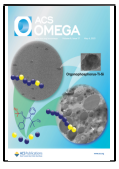

https://doi.org/10.1021/acsomega.1c01094
ACS Omega 2021, 6, 11750−11755

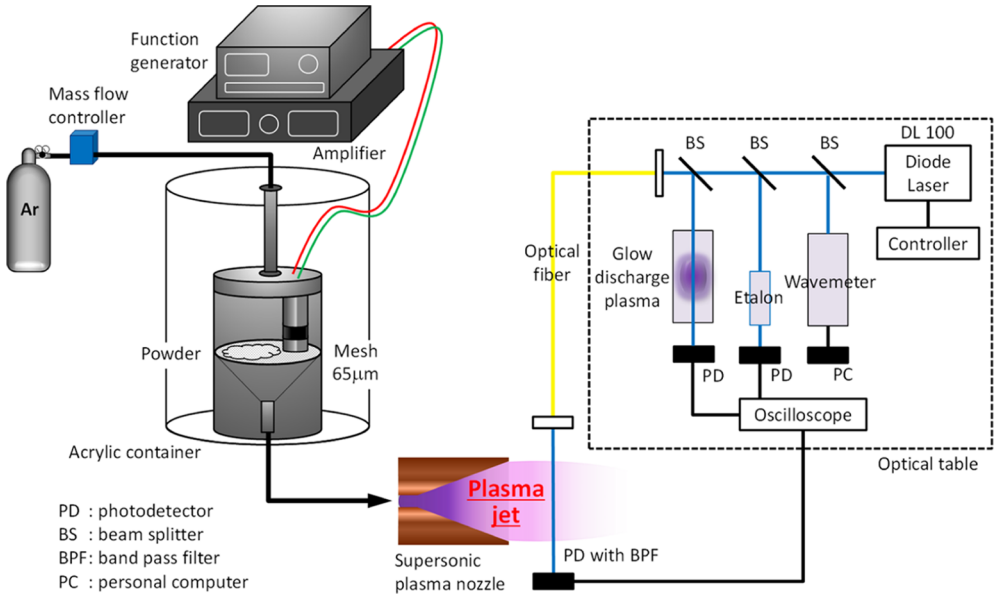

Figure 1. Schematic of the developed instrument. Strontium powder was fed upstream of the supersonic nozzle using an ultrasonic sieving machine with Ar gas.

atoms emitted into a plasma plume reach 5000−10,000 K.[9,17−19] Thus, the isotope shift of ^{88}Sr−^{90}Sr, 206.2 MHz, cannot be distinguished via LAAS due to an increase in the Doppler broadening under such high-temperature conditions.[20] Considering natural broadening, the residual of the Doppler broadening must be suppressed to less than 180 MHz in the half width at half-maximum. This is equivalent to approximately 60 K in the translational temperature.

We recently developed a novel analytical instrument that combined the high-temperature region for sample atomization with the low-temperature region for isotopic identification in a single unit.[21,22] In our previous study, only stable Xe isotopes in the gaseous phase were investigated. Notably, a dramatic reduction in the temperature of the Xe atoms to approximately 180 K was achieved. The Xe isotope analysis was verified through comparison with the naturally abundant variant. Nevertheless, to apply this methodology to solid samples, the atomization process must be considered. Several studies have proposed numerical modeling and qualitative spectroscopic measurements using emission spectroscopy in the field of materials processing; however, quantification of the atomization efficiency, which is defined as the number of evaporated atoms divided by the number of atoms in powdered molecules, requires further investigation.[23,24]

In the current study, a novel instrument for the direct analysis of solid samples containing strontium (Sr) isotopes is described. We obtained absorption spectra at 460.7 nm using diode laser absorption spectroscopy (DLAS) in a supersonic plasma jet while feeding $SrCl_2$ powder upstream of the supersonic nozzle. The drastic change in the temperature of the evaporated Sr atoms and the improvement in the wavelength resolution were examined. The atomization efficiency was determined based on the measured atomic number density and flow velocity.

MATERIALS AND METHODS

Figure 1 illustrates the experimental setup used in this study. The system comprised three key components: atomizer, sample feeder, and laser spectroscopy regions.

Arc-heated plasma was generated between electrodes upstream of the supersonic nozzle, that is, in the atomization section, in which the powder sample was fed from the sample feeding section via a carrier gas. Laser spectroscopy measurements were performed in the supersonic plasma jet in the third region, in which the temperature dramatically decreased due to the conversion of energy from thermal to kinetic.

The main components of the atomization section included a thoriated W cathode, a water-cooled Cu anode, and a brass expansion nozzle. The vacuum chamber was connected to a vacuum-pumping system, which comprised a rotary pump (SR-3700B, Osaka Vacuum, Ltd., Japan) and a mechanical booster pump (RA1200, Shinko Seiki, Japan). The description of the supersonic nozzle has been reported in our previous study.[21]

In this study, an ultrasonic sieving machine was used as the powder feeder, in which the ultrasonic vibration was generated using a bolt-clamped Langevin-type ultrasonic actuator (HEC-1540P2BF, Honda Electronics Co., Ltd., Japan) based on a piezoelectric element. The powder feed rate was tuned by adding an ultrasonic signal to the piezoelectric element. The feed rate was calibrated under atmospheric conditions (Figure S1).

$SrCl_2{\cdot}6H_2O$ (FUJIFILM Wako Pure Chemical, Japan) was used as the powder sample. The W electrode can get damaged by the atomic oxygen generated upstream of the nozzle. Additionally, hygroscopicity can disturb the stable powder feed by increasing the particle size. Thus, the powder sample was first dehydrated by heating. The variation in the powder mass following heating is shown in Figure S2.

The line width of the external cavity diode laser (DL100, Toptica Photonics, Germany) was approximately 100 kHz. The laser wavelength was scanned by modulating the grating and laser operating current using a ramp function and was monitored using a wavemeter (WS6-600, HighFinesse GmbH, Germany). The relative laser wavelength was calibrated using an optical cavity comprising two highly reflective mirrors (PSCM95-25.4C6.35-1000-460, Sigma Koki, Japan) installed in the free space. The repetition frequency was approximately 1 Hz, while the width of the scanning frequency was

https://doi.org/10.1021/acsomega.1c01094
ACS Omega 2021, 6, 11750−11755

approximately 10 GHz. The intensity of the incident laser beam was set to a low power (<10 μW) to prevent broadening of the spectral width due to absorption saturation. To measure the flow velocity, the laser beam was transmitted at the plane 3 mm downstream of the nozzle exit with an incident angle of 80° with respect to the flow axis.

The transmitted laser beams were detected using photodetectors (DET10/M, Thorlabs, USA), and their voltage signals were recorded using an oscilloscope (DL850E, Yokogawa, Japan) with a 12-bit resolution at a maximum sampling rate of 10 MS·s^{-1}. In addition to Sr detection, DLAS measurements of Ar atoms were simultaneously conducted to measure the flow velocity to determine the mass flow rate of the Sr atoms downstream of the nozzle. The spatial number density distribution of Sr atoms in the ground state exhibited a peak at a position away from the central axis of the plasma jet. Therefore, the flow velocity evaluated based on the Sr atoms might be underestimated compared with that found based on the Ar atoms.[25]

RESULTS AND DISCUSSION

The resonance line of Sr I 460.73 nm (Sr I, 5s^2 ^{1}S$_0$−5s5p ^{1}P$_1$) was selected based on the detection sensitivity because in the low-temperature plasma, almost all atoms existed in the ground state.[26] The operating conditions of the arc-heated plasma wind tunnel are summarized in Table 1.

Table 1. Operating Conditions of the Supersonic Plasma Jet

parameters	values
current	60 A
voltage	18−25 V
argon mass flow rate	0.13 g·s^{-1}
ambient pressure	30 Pa
plenum pressure	89 kPa

Sr Detection and Temperature Reduction. The absorption spectra were broadened via certain physical mechanisms in the plasmas (Figure 2a). Such a profile can be expressed using the following Voigt function: $V(\nu) = \int_{-\infty}^{\infty} G(\delta)L(\nu - \delta)\mathrm{d}\delta$. Notably, it is a convolution of the Gaussian function $G(\nu)$ and Lorentz function $L(\nu)$. In the glow discharge plasma, Doppler broadening was dominant compared to other broadenings described by the Lorentz function. The operating conditions of the glow discharge plasma are listed in Table S2. Thus, the translational temperature was evaluated using the Gaussian function. Moreover, as the influence of the natural broadening is not negligible in a low-temperature plasma, the Voigt function must be considered. The absorption coefficient can be described using the following equation

$$k(\nu) = \frac{k_0}{\pi\Delta\nu_L}\int_{-\infty}^{\infty}\frac{\exp\left\{-\left(\frac{\delta}{\sqrt{2}\sigma}\right)^2\right\}}{1+\left\{\frac{(\nu-\nu_0-\delta)}{\Delta\nu_L}\right\}^2}\mathrm{d}\delta \quad (1)$$

where k_0 is the absorption coefficient at the center frequency, σ is the standard deviation of the Gaussian function, $\Delta\nu_L$ is the sum of the half width at half-maximum of the Lorentz function, and δ is the integration variable.[27] In addition, considering the isotope effects of four natural isotopes (i.e., ^{84}Sr, ^{86}Sr, ^{87}Sr, and ^{88}Sr), the absorption coefficient can be expressed by

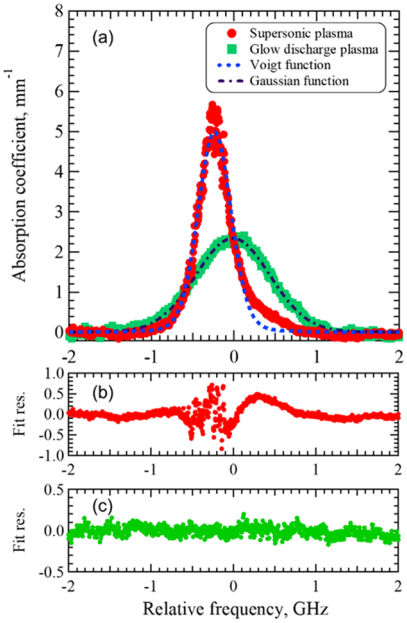

Figure 2. (a) Typical absorption spectra of Sr atoms in the supersonic plasma jet and glow discharge plasma. (b) Fitting residuals of the spectrum in the supersonic plasma jet. (c) Fitting residuals of the spectrum in the glow discharge plasma.

$$k_{Sr}(\nu) = \sum_{i=0}^{4}\frac{R_i k_0}{\pi\Delta\nu_L}\int_{-\infty}^{\infty}\frac{\exp\left\{-\left(\frac{\delta}{\sqrt{2}\sigma}\right)^2\right\}}{1+\left\{\frac{(\nu-\nu_0-\Delta\nu_i-\delta)}{\Delta\nu_L}\right\}^2}\mathrm{d}\delta \quad (2)$$

where $\Delta\nu_i$ is the isotope shift, while R_i denotes the abundance ratio. These parameters are summarized in Table S1.

In this study, the curve fittings to the Voigt functions were performed using the SciPy library, which is an open-source software in Python. Here, the temperatures were calculated solely from the Doppler width, assuming that the Lorentz width was constant. The full width at half-maximum ($A/2\pi$) of 32 MHz was calculated using the Einstein coefficient, that is, $A = 2.01 \times 10^8$.[28]

The absorption spectrum of Sr atoms observed in the supersonic plasma jet was narrower than the spectrum detected in the glow discharge plasma (Figure 2a); the former was in good agreement with the Voigt function (Figure 2a,b). The residuals at the tail area were attributed to fluctuations of the probe laser beam caused by mechanical vibration. The translational temperature was determined using the standard deviation of the Gaussian function according to the following equation

$$T = \frac{M_A}{k_B}\lambda_0^2\sigma^2 \quad (3)$$

where M_A refers to the atomic mass, k_B denotes the Boltzmann constant, λ indicates the center wavelength of an absorption line, and σ is the standard deviation of the Gaussian function. The half width at half-maximum of the Doppler broadening was obtained as 230 MHz using $\Delta\nu_D = \sqrt{2\ln 2}\,\sigma$, where σ is the standard deviation of the Gaussian function. In addition, the corresponding temperature was 85.2 K. The sum of the Doppler and Lorentz widths was 246 GHz. By reducing the

https://doi.org/10.1021/acsomega.1c01094
ACS Omega 2021, 6, 11750−11755

temperature, we successfully narrowed the spectral linewidth to a width comparable to the isotope shift of $^{88}Sr-^{90}Sr$.[20] The temperature reduction of Sr atoms was due to two factors. The first is due to adiabatic expansion by a supersonic nozzle. Second, a further temperature reduction occurs due to the temperature difference between two species of mixed gas. The temperature of Ar atoms measured simultaneously was 1410 K, and a temperature difference between the Sr and Ar atoms was observed. As described in our previous study, this difference is caused by the energy level of the lower state being used for the absorption transition, which results in a line integral of the absorption coefficient.[29] Thus, accessing a ground state has the effect of reducing the temperature compared with using an absorption transition from an excited state.

Sr Number Density and Atomization Efficiency. The total number density of Sr atoms can be directly evaluated based on an absorption line from the ground state. In general, the number density can be determined using the integral of the absorption coefficient over the frequency according to the following equation

$$n_{Sr} = \frac{8\pi}{\lambda^2}\frac{g_i}{g_j}A_{ji}\int_{-\infty}^{\infty} k(\nu)\mathrm{d}\nu \tag{4}$$

where i and j are the lower and upper energy levels, respectively. The relationship between the number density of Sr atoms in the ground state and the ultrasonic sieving voltage is shown in Figure 3. Here, the absorption length was assumed to be 30 mm, which is the diameter of the nozzle exit.

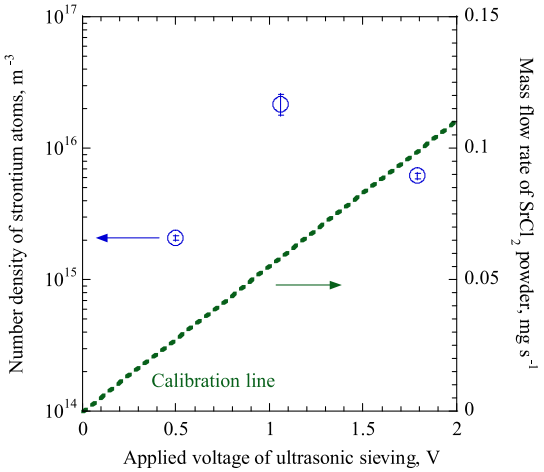

Figure 3. Number density of Sr atoms in the ground state and the calibration line of the mass flow rate of the $SrCl_2$ powder. Error bars represent standard deviations.

The maximum value of the Sr number density in the plasma jet was 2.54×10^{16} m^{-3} at a sieving voltage of 1.0 V. By calculating the number density of the Ar atoms from the equation of state (1.54×10^{21} m^{-3}), the concentration of Sr atoms in the plasma jet was 1.7 ppm. Moreover, the detection limit of the atomic Sr concentration in the developed analytical instrument was approximately 130 ppb, which corresponded to the 3σ criteria of 2.05×10^{14} m^{-3} in the atomic number density measured at a sieving voltage of 0.5 V.

For the direct analysis of solid samples, consideration of the atomization efficiency parameter is important to enhance quantification and sensitivity. In this study, the atomization efficiency was evaluated using the ratio of the mass flow rate of the Sr atoms in the plasma jet to the mass flow rate of the $SrCl_2$ powder multiplied by the weight fraction of the Sr atoms. Thus, the atomization efficiency can be defined by the following equation

$$\eta = \frac{\dot{m}_{atom}}{\dot{m}_{powder}} \tag{5}$$

Additionally, the mass flow rate of the Sr atoms in the plasma jet can be calculated using the measured number density and flow velocity according to the following relationship

$$\dot{m}_{atom} = \rho \cdot A \cdot V = n_{Sr} \cdot M_A \cdot S \cdot V \tag{6}$$

where S is the cross section of the plasma jet calculated from the diameter of the nozzle exit, that is, 30 mm, while V refers to the flow velocity determined by the Ar atoms. The absorption spectra of the Ar atoms in the supersonic plasma jet and in the glow discharge plasma as the reference cell are illustrated in Figure S4.

The maximum value of the atomization efficiency was 10.4 ± 1.8% at a powder mass rate of 0.06 mg·s^{-1} (Figure 4).

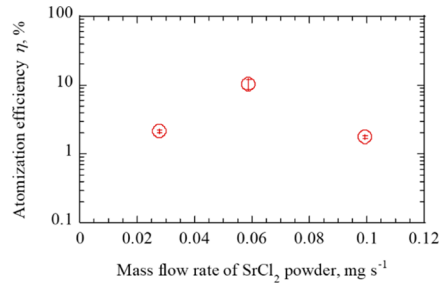

Figure 4. Atomization efficiency of the $SrCl_2$ powder. Error bars represent standard deviations.

Temporal fluctuations in the mass flow rate of the Sr atoms in the supersonic plasma jet caused instability in the atomization efficiency. Meanwhile, the temperature and flow velocity in the supersonic plasma jet obtained from Ar atoms varied in the range of 1410 ± 200 K and 1520 ± 90 m/s, respectively. When the total enthalpies were converted to upstream temperatures by using the equation described in the Supporting Information, these changes were in the range of approximately 700 K.[30] The calculated absolute temperatures were lower than the true values on the central axis unless the radial temperature distribution was obtained via Abel inversion. Although the temperature upstream of the nozzle reported in our previous study (6490 K) was significantly higher than the boiling point of $SrCl_2$ (1520 °C), the results obtained herein indicated that the powder was not sufficiently heated due to the short residence time and narrow temperature distribution upstream of the nozzle.[31] Thus, a swirl flow can increase the residence time of powder particles and carrier gas.

CONCLUSIONS

Employing an ultrasonic sieve as a powder feeder, the direct detection of Sr atoms from the $SrCl_2$ powder in a supersonic plasma jet was conducted using DLAS for a resonance line Sr I 460.7 nm. The detection limit of the Sr atoms was approximately 130 ppb in Ar gas, and the translational temperature of the Sr atoms was successfully reduced to 85.2 K by adiabatic expansion and the effect of the temperature

https://doi.org/10.1021/acsomega.1c01094
ACS Omega 2021, 6, 11750−11755

difference. Furthermore, using the number density of the Sr atoms measured via DLAS, we demonstrated that 10.4% of the Sr atoms in the powder sample was vaporized during the atomization process employing a supersonic plasma wind tunnel.

The results obtained herein indicate the suitability of the developed methodology for direct atomization without the necessity for complex sample preparation. Moreover, our approach exhibits an improved wavelength resolution. The obtained low-temperature plasma enables slight isotope shifts of medium heavy elements. However, the current study was conducted under a limited and narrow range of experimental conditions. Hence, the plasma conditions, including the swirl flow generation, should be optimized to further enhance the wavelength resolution and atomization efficiency. Further experiments must be conducted using a higher feed range and different particle sizes.

■ ASSOCIATED CONTENT

Supporting Information

The Supporting Information is available free of charge at https://pubs.acs.org/doi/10.1021/acsomega.1c01094.

Details of the isotope shifts and abundance ratio used in the curve fitting, calibration curves of the powder mass flow rate, time variation of the powder mass after dehydration treatment, typical absorption spectra of Ar atoms in an excited state, and calculation of the total enthalpy of a supersonic plasma jet (PDF)

■ AUTHOR INFORMATION

Corresponding Author

Akira Kuwahara − *Department of Applied Energy, Nagoya University, Aichi 464-8603, Japan; Department of Decommissioning and Waste Management, Japan Atomic Energy Agency, Ibaraki 319-1195, Japan;* orcid.org/0000-0001-5694-3532; Phone: +81 52 789 5936; Email: akuwahara@energy.nagoya-u.ac.jp

Authors

Yasuaki Aiba − *Department of Engineering, Shizuoka University, Shizuoka 432-8561, Japan*

Makoto Matsui − *Department of Engineering, Shizuoka University, Shizuoka 432-8561, Japan*

Complete contact information is available at: https://pubs.acs.org/10.1021/acsomega.1c01094

Author Contributions

A.K. and M.M. designed the research project, A.K. and Y.A. performed experiments and analyzed data, and A.K. and M.M. wrote and edited the manuscript.

Notes

The authors declare no competing financial interest.

■ ACKNOWLEDGMENTS

This study was supported in part by JSPS KAKENHI Grant-in-Aid for Early-Career Scientists (Grant No.: 18K14162) and Scientific Research(B) (Grant No.: 21H01858).

■ REFERENCES

(1) Croudace, I. W.; Russell, B. C.; Warwick, P. W. Plasma source mass spectrometry for radioactive waste characterisation in support of nuclear decommissioning: a review. *J. Anal. At. Spectrom.* **2017**, *32*, 494−526.

(2) Becker, J. S. Mass spectrometry of long-lived radionuclides. *Spectrochim. Acta, Part B* **2003**, *58*, 1757−1784.

(3) Becker, J. S. Inductively Coupled Plasma Mass Spectrometry (ICP-MS) and Laser Ablation ICP-MS for Isotope Analysis of Long-lived Radionuclides. *Int. J. Mass Spectrom.* **2005**, *242*, 183−195.

(4) Valković, V. *Radioactivity in the Environment*, 2nd ed.; Elsevier: Amsterdam, 2019.

(5) Kavasi, N.; Sahoo, S. K.; Arae, H.; Aono, T.; Palacz, Z. Accurate and Precise Determination of ^{90}Sr at Femtogram Level in IAEA Proficiency Test Using Thermal Ionization Mass Spectrometry. *Sci. Rep.* **2019**, *9*, 1653.

(6) Warwick, P. E.; Russell, B. C.; Croudace, I. W.; Zacharauskas, Ž. Evaluation of Inductively Coupled Plasma Tandem Mass Spectrometry for Radionuclide Assay in Nuclear Waste Characterisation. *J. Anal. At. Spectrom.* **2019**, *34*, 1810−1821.

(7) Takagai, Y.; Furukawa, M.; Kameo, Y.; Suzuki, K. Sequential inductively coupled plasma quadrupole mass-spectrometric quantification of radioactive strontium-90 incorporating cascade separation steps for radioactive contamination rapid survey. *Anal. Methods* **2014**, *6*, 355−362.

(8) Quentmeier, A.; Bolshov, M.; Niemax, K. Measurement of uranium isotope ratios in solid samples using laser ablation and diode laser-atomic absorption spectrometry. *Spectrochim. Acta, Part B* **2001**, *56*, 45−55.

(9) Liu, H.; Quentmeier, A.; Niemax, K. Diode Laser Absorption Measurement of Uranium Isotope Ratios in Solid Samples Using Laser Ablation. *Spectrochim. Acta, Part B* **2002**, *57*, 1611−1623.

(10) Miyabe, M.; Oba, M.; Jung, K.; Iimura, H.; Akaoka, K.; Kato, M.; Otobe, H.; Khumaeni, A.; Wakaida, I. Laser ablation absorption spectroscopy for isotopic analysis of plutonium: Spectroscopic properties and analytical performance. *Spectrochim. Acta, Part B* **2017**, *134*, 42−51.

(11) Srivastava, A.; Hodges, J. T. Development of a High-Resolution Laser Absorption Spectroscopy Method with Application to the Determination of Absolute Concentration of Gaseous Elemental Mercury in Air. *Anal. Chem.* **2018**, *90*, 6781−6788.

(12) Qu, Z.; Steinvall, E.; Ghorbani, R.; Schmidt, F. M. Tunable Diode Laser Atomic Absorption Spectroscopy for Detection of Potassium under Optically Thick Conditions. *Anal. Chem.* **2016**, *88*, 3754−3760.

(13) Jacquet, P.; Pailloux, A. Laser Absorption Spectroscopy for Xenon Monitoring in the Cover Gas of Sodium Cooled Fast Reactors. *J. Anal. At. Spectrom.* **2013**, *28*, 1298−1302.

(14) Wang, C. Plasma-cavity Ringdown Spectroscopy (P-CRDS) for Elemental and Isotopic Measurements. *J. Anal. At. Spectrom.* **2007**, *22*, 1347−1363.

(15) Hou, H.; Chan, G. C.-Y.; Mao, X.; Zorba, V.; Zheng, R.; Russo, R. E. Femtosecond Laser Ablation Molecular Isotopic Spectrometry for Zirconium Isotope Analysis. *Anal. Chem.* **2015**, *87*, 4788−4796.

(16) Miyabe, M.; Oba, M.; Iimura, H.; Akaoka, K.; Maruyama, Y.; Ohba, H.; Tampo, M.; Wakaida, I. Doppler-shifted Optical Absorption Characterization of Plume-lateral Expansion in Laser Ablation of a Cerium Target. *J. Appl. Phys.* **2012**, *112*, 123303.

(17) Verhoff, B.; Harilal, S. S.; Freeman, J. R.; Diwakar, P. K.; Hassanein, A. Dynamics of Femto- and Nanosecond Laser Ablation Plumes Investigated Using Optical Emission Spectroscopy. *J. Appl. Phys.* **2012**, *112*, 093303.

(18) Harilal, S. S.; Lahaye, N. L.; Phillips, M. C. High-resolution Spectroscopy of Laser Ablation Plumes Using Laser-induced Fluorescence. *Opt Express* **2017**, *25*, 2312−2326.

(19) Harilal, S. S.; Murzyn, C. M.; Phillips, M. C.; Martin, J. B. Hyperfine structures and isotopic shifts of uranium transitions using tunable laser spectroscopy of laser ablation plumes. *Spectrochim. Acta, Part B* **2020**, *169*, 105828.

(20) Martin, A. G.; Dutta, S. B.; Rogers, W. F.; Clark, D. L. Measurement of the optical isotope shift ofSr82. *Phys. Rev. C* **1986**, *34*, 1120−1122.

(21) Kuwahara, A.; Aiba, Y.; Nankawa, T.; Matsui, M. Development of an Isotope Analysis Method Based on Diode Laser Absorption Spectroscopy Using an Arc-jet Plasma Wind Tunnel. *J. Anal. At. Spectrom.* **2018**, *33*, 893−896.
(22) Kuwahara, A.; Aiba, Y.; Yamasaki, S.; Nankawa, T.; Matsui, M. High Spectral Resolution of Diode Laser Absorption Spectroscopy for Isotope Analysis Using a Supersonic Plasma Jet. *J. Anal. At. Spectrom.* **2018**, *33*, 1150−1153.
(23) Buchner, P.; Ferfers, H.; Schubert, H.; Uhlenbusch, J. Evaporation of copper powders in an inductively coupled thermal rf plasma - numerical modelling and spectroscopic measurements. *Plasma Sources Sci. Technol.* **1997**, *6*, 450−459.
(24) Shin, J. W.; Miyazoe, H.; Leparoux, M.; Siegmann, S.; Dorier, J. L.; Hollenstein, C. The influence of process parameters on precursor evaporation for alumina nanopowder synthesis in an inductively coupled rf thermal plasma. *Plasma Sources Sci. Technol.* **2006**, *15*, 441−449.
(25) Makoto, M.; Takayanagi, H.; Oda, Y.; Komurasaki, K.; Arakawa, Y. Performance of Arcjet-type Atomic-oxygen Generator by Laser Absorption Spectroscopy and CFD Analysis. *Vacuum* **2003**, *73*, 341−346.
(26) Shimada, Y.; Chida, Y.; Ohtsubo, N.; Aoki, T.; Takeuchi, M.; Kuga, T.; Torii, Y. A Simplified 461-nm Laser System Using Blue Laser Diodes and a Hollow Cathode Lamp for Laser Cooling of Sr. *Rev. Sci. Instrum.* **2013**, *84*, 063101.
(27) Matsui, M.; Tanaka, K.; Nomura, S.; Komurasaki, K.; Yamagiwa, Y.; Arakawa, Y. Generation and diagnostics of atmospheric pressure CO2 plasma by laser driven plasma wind tunnel. *J. Appl. Phys.* **2012**, *112*, 033301.
(28) NIST. NIST Standard Reference Database 78. http://webbook.nist.gov/pml/atomic-spectra-database (accessed December 29, 2020).
(29) Kuwahara, A.; Aiba, Y.; Nankawa, T.; Matsui, M. Temperature Difference Between Gas Species In Absorption Measurements Using Diode Laser Absorption Spectroscopy And The Effect On Temperature Reduction. *Atom. Spectros* **2021**, *42*. DOI: 10.46770/AS.2021.006.
(30) Zhang, F.-Y.; Komurasaki, K.; Iida, T.; Fujiwara, T. Diagnostics of an argon arcjet plume with a diode laser. *Appl. Opt.* **1999**, *38*, 1814−1822.
(31) Inoue, T.; Matsui, M.; Takayanagi, H.; Komurasaki, K.; Arakawa, Y. Effect of Swirl Flow on an Atmospheric Inductively Coupled Plasma Supersonic Jet. *Vacuum* **2006**, *80*, 1174−1178.

https://doi.org/10.1021/acsomega.1c01094
ACS Omega 2021, 6, 11750−11755